

1 **Programmable peroxidase-assisted signal amplification enables flexible detection of**  
2 **nucleic acid targets in cellular and histopathological specimens**

3  
4 Sahar Attar<sup>1,2</sup>, Valentino E. Browning<sup>1</sup>, Yuzhen Liu<sup>1</sup>, Eva K. Nichols<sup>1</sup>, Ashley F. Tsue<sup>4,5,6</sup>, David  
5 M. Shechner<sup>4,5,6</sup>, Jay Shendure<sup>1,5,6,7,8</sup>, Joshua A. Lieberman<sup>2</sup>, Shreeram Akilesh<sup>2,3\*</sup>, Brian J.  
6 Beliveau<sup>1,5\*</sup>

7  
8 <sup>1</sup>Department of Genome Sciences, University of Washington, Seattle, WA, USA

9  
10 <sup>2</sup>Department of Laboratory Medicine and Pathology, University of Washington, Seattle, WA,  
11 USA

12  
13 <sup>3</sup>Kidney Research Institute, Seattle, WA, USA

14  
15 <sup>4</sup>Department of Pharmacology, University of Washington, Seattle, WA, USA

16  
17 <sup>5</sup>Brotman Baty Institute for Precision Medicine, Seattle, WA, USA

18  
19 <sup>6</sup>Institute of Stem Cell and Regenerative Medicine, University of Washington, USA

20  
21 <sup>7</sup>Allen Discovery Center for Cell Lineage Tracing, Seattle, WA, USA

22  
23 <sup>8</sup>Howard Hughes Medical Institute, University of Washington, Seattle, WA, USA

24  
25  
26 \*Correspondence e-mail: [shreeram@uw.edu](mailto:shreeram@uw.edu); [beliveau@uw.edu](mailto:beliveau@uw.edu)

27  
28  
29  
30  
31  
32  
33  
34  
35  
36  
37  
38  
39  
40  
41  
42  
43  
44  
45  
46  
47  
48

1 **Abstract**

2 *In situ* hybridization (ISH) is a powerful tool for investigating the spatial arrangement of nucleic  
3 acid targets in fixed samples. ISH is typically visualized using fluorophores to allow high  
4 sensitivity and multiplexing or with colorimetric labels to facilitate co-visualization with  
5 histopathological stains. Both approaches benefit from signal amplification, which makes  
6 target detection effective, rapid, and compatible with a broad range of optical systems. Here,  
7 we introduce a unified technical platform, termed ‘pSABER’, for the amplification of ISH signals  
8 in cell and tissue systems. pSABER decorates the *in situ* target with concatemeric binding sites  
9 for a horseradish peroxidase-conjugated oligonucleotide which can then catalyze the massive  
10 localized deposition of fluorescent or colorimetric substrates. We demonstrate that pSABER  
11 effectively labels DNA and RNA targets, works robustly in cultured cells and challenging  
12 formalin fixed paraffin embedded (FFPE) specimens. Furthermore, pSABER can achieve 25-  
13 fold signal amplification over conventional signal amplification by exchange reaction (SABER)  
14 and can be serially multiplexed using solution exchange. Therefore, by linking nucleic acid  
15 detection to robust signal amplification capable of diverse readouts, pSABER will have broad  
16 utility in research and clinical settings.

17  
18  
19  
20  
21  
22  
23  
24  
25  
26  
27  
28  
29  
30  
31  
32  
33  
34  
35  
36  
37  
38  
39  
40  
41  
42  
43  
44  
45  
46  
47  
48

## 1 Introduction

2 Since its introduction by Pardue and Gall<sup>1</sup> in the late 1960s, *in situ* hybridization (ISH)  
3 has been widely used in research and clinical settings to determine the abundance and  
4 subcellular location of nucleic acid targets. ISH relies on the formation of heteroduplexes  
5 between target RNA and DNA strands present in fixed cellular and tissue samples and  
6 complementary probe strands that are added during a hybridization reaction. Once completed,  
7 the results of the hybridization reaction can be visualized using transmitted light or fluorescent  
8 microscopy depending on the type of labeling strategy used. Common applications for ISH  
9 include targeting intervals of genomic DNA to assay chromosome copy number in cytogenetic  
10 clinics<sup>2</sup>, the quantitative profiling of single-cell RNA expression profiles<sup>3</sup>, the investigation of  
11 how chromosomes are spatially organized within the nucleus<sup>4</sup>, and the visualization of gene  
12 expression patterns in whole mount tissue specimens<sup>5</sup>.

13 Considerable technical development has occurred to improve the sensitivity of ISH and  
14 to broaden its applications. Among these, notable developments include the transition from  
15 radioactive to fluorescent labels<sup>6-8</sup>, the use of recombinant<sup>9</sup> and synthetic<sup>3,10-13</sup> DNA as a source  
16 of probe material, and the introduction of massively multiplexed imaging approaches that rely  
17 on iterative rounds of hybridization and imaging in the same sample<sup>14-16</sup>. Another set of  
18 technical development has focused on strategies to amplify the signal of ISH, which has  
19 particular benefits in challenging sample types such as formalin-fixed, paraffin-embedded  
20 (FFPE) tissue sections, thick frozen tissue sections, and whole mount tissue samples<sup>17,18</sup>.  
21 Broadly, these signal amplification approaches fall into two categories: 1) Assembly-based  
22 technologies in which DNA and/or protein species are directed to the site(s) of ISH in order to  
23 create an *in situ* scaffold capable of recruiting many directly labeled molecules to increase the  
24 overall label density at the target site. Examples of assembly-based approaches include the  
25 assembly of branched DNA (bDNA)<sup>19,20</sup> and LNA<sup>21</sup> structures, hybridization chain reaction  
26 (HCR)<sup>22</sup>, and ClampFISH<sup>23,24</sup>; 2) Enzymatic approaches in which specialized probe sets recruit  
27 enzymes to catalyze the formation of signal amplification structures *in situ*. Examples of  
28 enzymatic approaches include the catalyzed reporter deposition (CARD) technique that uses  
29 the horseradish peroxidase (HRP) enzyme to locally deposit detectable biotin molecules<sup>25</sup>,  
30 methods that recruit HRP or alkaline phosphatase for colorimetric detection via haptene  
31 probes in whole-mount embryos<sup>26</sup>, and rolling circle amplification (RCA)<sup>27</sup>.

32 Assembly-based and enzymatic signal amplification approaches can strengthen signals  
33 by >100x, making it easier to detect analytes in thick and noisy sample types. These methods  
34 even make it possible to image labeled specimens on low numerical aperture imaging systems  
35 with lower photon collection efficiencies. However, as these approaches require that the signal  
36 amplification structure be created *in situ*, they can be difficult to troubleshoot, particularly for  
37 researchers who are performing ISH itself for the first time. Moreover, many of these  
38 approaches rely on costly or proprietary reagents, which adds to the difficulty of establishment  
39 and implementation. The recently developed signal amplification by exchange reaction  
40 (SABER) technique introduced by Kishi and colleagues<sup>28</sup> abrogates these issues, as signal  
41 amplification in SABER is achieved by the *in vitro* addition of long, concatemeric ssDNA tails to  
42 the probe molecules via the primer exchange reaction (PER)<sup>29</sup> prior to their addition to the fixed  
43 sample. As the creation of the signal amplification structure occurs *in vitro*, researchers can  
44 evaluate the results of the PER reaction and troubleshoot as needed prior to executing time  
45 consuming ISH experiments with precious samples. In addition to this useful feature, SABER  
46 has many strong attributes as a signal amplification approach, including low-cost (\$1–5 per  
47 sample) simple and robust multiplexing via solution exchange<sup>28</sup>.

48 While SABER has features that may accelerate its adoption, it still has limitations. For  
49 instance, SABER can achieve ~450x signal amplification when it employs iterative rounds of

1 branched assembly *in situ*<sup>28</sup>, but to date that approach has only been shown for imaging one  
2 target at a time and has only been used on cultured cells, and the unbranched form of SABER  
3 that supports multicolor imaging in cells and tissues only provides a more modest ~5–15x  
4 amplification<sup>28</sup>. SABER also has yet to be combined with colorimetric detection methods,  
5 which facilitate co-visualization with histopathological stains such as hematoxylin and eosin.  
6 Here, we introduce ‘peroxidase-SABER’ (pSABER), a robust and cost-effective strategy for  
7 boosting the signal of SABER by a further 20-fold and expanding its readout modalities to  
8 include colorimetric detection. We demonstrate the effectiveness of colorimetric and  
9 fluorescent pSABER in fixed cells and FFPE tissue sections and showcase the ability of  
10 pSABER to perform highly amplified and multiplexed imaging via solution exchange. We  
11 anticipate that its simplicity and its seamless integration into the existing SABER toolkit will  
12 lead to the adoption of pSABER as a workhorse technique for *in situ* nucleic acid detection in  
13 research and clinical settings.

14  
15

## 16 **Results**

17

### 18 **Programing enzymatic signal amplification with pSABER**

19 The pSABER approach builds on the established, unbranched SABER workflow. First,  
20 probe sets or “readout oligos” complementary to a common exogenous binding site encoded  
21 in complex oligo probe libraries are extended *in vitro* by the primer exchange reaction  
22 (PER)<sup>28,29</sup>, resulting in the addition of long concatemers of a reiterated 10 nt PER sequence (Fig.  
23 1). These concatemers are then applied to the sample and primary *in situ* hybridization is  
24 performed (and secondary hybridization with extended readout oligos in the case that readout  
25 oligos are being used). To detect the hybridized concatemers, the sample is then hybridized  
26 with a 20 nt oligo covalently conjugated to HRP that is complementary to a dimer of the  
27 reiterated PER sequence (Fig. 1). Finally, the sample is incubated with H<sub>2</sub>O<sub>2</sub> and an HRP  
28 substrate to facilitate the localized deposition of a variety of colorimetric or fluorescent labels  
29 that can be detected by microscopy (Fig. 1).

30

### 31 **pSABER enables amplified colorimetric detection**

32 In order to validate the pSABER approach and demonstrate its compatibility with  
33 colorimetric detection, we designed a series of RNA and DNA ISH experiments against well-  
34 established molecular targets. We first performed an RNA ISH experiment using a probe set  
35 consisting of 83 oligos targeting the *ADAMTS1* mRNA in human K29Mes cells that had been  
36 shifted to 37°C prior to fixation to induce *ADAMTS1* expression<sup>30</sup>. After primary hybridization,  
37 the sample was developed with 3,3'-Diaminobenzidine (DAB) in the presence of H<sub>2</sub>O<sub>2</sub> prior to  
38 hematoxylin staining and mounting. Upon visualization by routine brightfield microscopy, both  
39 robust cytoplasmic DAB staining consistent with single-molecule RNA FISH<sup>3</sup> and strong  
40 nuclear puncta corresponding to sites of induced transcription<sup>30</sup> were observed, neither of  
41 which was visible in the no primary probe negative control (Fig. 2a). To test the applicability of  
42 pSABER to more challenging DNA ISH applications, we performed experiments targeting the  
43 human alpha satellite repeat DNA region in K29Mes cells (Fig. 2b) as well as a 200 kb single-  
44 copy chromosomal region on Xp22.32 (hg38 chrX:5400000–5600000) using a previously  
45 validated complex oligo library and an accompanying readout probe<sup>31</sup> on primary human  
46 metaphase chromosome spreads (Fig. 2c). In both cases, brightfield microscopy revealed  
47 strong, punctate staining in the expected patterns specific to DNA, whereas no appreciable  
48 staining was observed in the corresponding no primary probe controls (Fig. 2b,c). Finally, we  
49 examined the ability of colorimetric pSABER to detect targets in FFPE tissue sections, which

1 represents the main specimen format in clinical and research pathology laboratories  
2 worldwide. We first performed RNA ISH in deidentified human kidney FFPE sections using a  
3 probe set consisting of 6 oligos targeting the internal transcribed spacer 1 (ITS1) region of the  
4 47S pre-rRNA that is localized exclusively in the nucleolus<sup>32</sup>. After colorimetric development,  
5 we observed tightly localized signal inside of nearly every nucleus in the section, with the  
6 expected 1–2 signals per nucleus being observed (Fig. 2d). We also verified colorimetric RNA  
7 pSABER can detect RNA originating from a non-repetitive locus in FFPE specimens by  
8 performing RNA ISH with a probe set consisting of 83 oligos targeting the *UMOD* mRNA in  
9 deidentified human kidney sections. Using pSABER we detected a very specific pattern of  
10 *UMOD* transcript localization in cells of the thick ascending loop of Henle (TALH) (arrowheads,  
11 Fig. 2e, center panel), but not in cells of the adjacent macula densa (MD), a specialized  
12 structure in the vicinity of the kidney glomerulus-tubule junction. This localization pattern  
13 exactly matched *UMOD* protein expression as determined by immunohistochemistry in the  
14 human protein atlas<sup>33</sup>. No detectable staining was observed in the corresponding no primary  
15 probe controls for the kidney FFPE experiments (Fig. 2d,e). These experiments further  
16 validated pSABER for *in situ* localization of mRNA molecules in clinically relevant samples.  
17

### 18 **Enhanced signal amplification with fluorescent pSABER**

19 HRP can also catalyze covalent deposition of fluorophore-conjugated tyramides in a  
20 variety of specimen types. Therefore, we next set out to determine whether pSABER could  
21 generate amplified fluorescent signals *in situ* via the HRP-catalyzed deposition of fluorophore-  
22 conjugated tyramides at the sites of primary probe binding. To this end, we performed a series  
23 of fluorescent RNA pSABER experiments in EY.T4<sup>34</sup> mouse embryonic fibroblast cells using  
24 fluorescein-tyramide (Methods). During the development step, we independently targeted each  
25 of three RNA species with distinct expected spatial signal patterns: 1) the 47S rRNA ITS1  
26 region that is localized exclusively in the nucleolus<sup>32</sup> (Fig. 3a); 2) the 7SK small nuclear RNA  
27 which is broadly localized within the nucleoplasm and enriched in nuclear speckles, but  
28 excluded from nucleoli<sup>35</sup> (Fig. 3b); the *Cbx5* mRNA which localizes predominantly in the  
29 cytoplasm<sup>28</sup> (Fig. 3c). In all three cases, using confocal microscopy, we observed the expected  
30 staining patterns, whereas we saw no detectable signal in the no primary probe negative  
31 control (Fig. 3b). We also validated that fluorescent pSABER can faithfully visualize nucleic acid  
32 targets in FFPE specimens by performing an experiment targeting ITS1 in deidentified human  
33 kidney FFPE tissue sections. This revealed the expected pattern of strong nucleolar staining  
34 (Fig. 3e) that matched the signal seen with colorimetric DAB development (Fig. 2d) and that  
35 was not observed in the matched no primary probe negative control (Fig. 3f).  
36

37 After verifying that pSABER is readily compatible with fluorescent detection, we next  
38 set out to quantify the degree of signal amplification provided by pSABER. In particular, we  
39 aimed to measure how much, if any, additional amplification pSABER provides over the  
40 conventional version of the SABER technique. To this end, we performed a paired series of ISH  
41 experiments targeting the centromeric mouse minor satellite repeat in EY.T4 MEF cells in  
42 which the same pool of PER-extended probe was hybridized and visualized either via the  
43 recruitment of an ATTO 488 labeled oligo (SABER) or via the recruitment of an HRP-oligo  
44 followed by development with fluorescein-tyramide (pSABER) (Fig. 4a). Both samples were  
45 acquired using matched illumination and camera exposure settings. These settings were  
46 optimized to utilize the full dynamic range of the camera without significant amounts of pixel  
47 saturation (Methods), allowing a direct and quantitative comparison of the signal intensities of  
48 each sample (Fig. 4b). Following automated segmentation nuclei and minor satellite FISH  
49 puncta (Methods), pSABER was observed to produce a distribution of peak signal intensity per  
puncta values whose median was 25.1x greater than the corresponding SABER distribution

1 (Fig. 4c). A similar fold-enhancement (21.3x) was observed when comparing the means of the  
2 distributions (Fig. 4c). From these data, we conclude that fluorescent pSABER provides  
3 substantial signal amplification (>20x) relative to conventional SABER. Furthermore, as SABER  
4 was reported to produce ~10x signal amplification relative to unamplified FISH at similar  
5 targets<sup>28</sup>, we estimate that fluorescent pSABER provides >200x amplification relative to  
6 unamplified FISH.

### 7 8 **Exchange-pSABER for multiplexed detection with amplification**

9 A powerful feature of SABER is its ability to sequentially visualize multiple targets via  
10 the programmable displacement of bound fluorescently labeled oligos and the subsequent  
11 hybridization of labeled oligos to distinct targets bearing orthogonal sequence extensions<sup>28</sup>. We  
12 reasoned that fluorescent pSABER could also harness this property to enable multiplexed and  
13 highly amplified imaging via solution exchange of HRP-oligos between subsequent rounds of  
14 signal development (Fig. 5a). To test this idea, we designed a 3-color imaging experiment  
15 targeting the *Cbx5* mRNA, the 7SK small nuclear RNA, and the ITS1 region of the 47S rRNA. In  
16 this experiment, all primary probes were first co-hybridized in a single overnight step. Next, we  
17 added the HRP-oligo complementary to the “p27” SABER extension borne by the *Cbx5* probe  
18 set and developed this with Cy5-tyramide (Fig. 5b, top). We then removed the bound HRP-  
19 oligo by solution exchange into formamide buffer<sup>28</sup> (Methods), allowing us to perform a second  
20 round of hybridization of with the HRP-oligo, but this time complementary to the “p30”  
21 extension borne by the 7SK probe set and developed with Cy3-tyramide (Fig. 5b, middle). In  
22 the final cycle, we removed the bound HRP-oligo via solution exchange and performed a third  
23 round of hybridization and development at ITS1 with fluorescein-tyramide (Fig. 5c, bottom).  
24 Visualization after each round of development revealed the sequential accumulation of  
25 amplified signal patterns at the three targets, with the fluorescent tyramides added during  
26 previous rounds remaining stable and prominently visible even during later rounds (Fig. 3b).  
27 After the three rounds, we observed that signal associated with each RNA target was properly  
28 localized to the correct subcellular location with minimal spatial overlap even when visualized  
29 using “SoRa” super-resolution spinning disc confocal microscopy (Fig. 3c). Moreover, we  
30 found that we could observe the amplified, multiplexed staining pattern even when using lower  
31 numerical aperture air objectives on an automated slide scanning microscope at 40x, 20x and  
32 even 10x magnifications (Fig. 4d), whereas we were essentially unable to detect conventional  
33 SABER using the same system (Supplementary Fig. 1).

### 34 35 36 **Discussion**

37 The pSABER approach sits conveniently upon the established PER/SABER platform to  
38 expand its capabilities to colorimetric detection and highly amplified (>200x) multiplexing at up  
39 to three molecular targets. The use of an HRP-oligo integrates seamlessly into the SABER FISH  
40 workflow and only adds a brief (~10 min) hydrogen peroxide incubation prior to sample  
41 permeabilization to inactive endogenous peroxidases and a short series of washes (~10-30  
42 mins) after development by HRP to remove residual HRP substrate. The use of the HRP-oligo  
43 and tyramide substrates is effectively cost-equivalent to performing conventional SABER,  
44 increasing the cost of visualization reagents per sample from ~\$0.10–\$0.60 per sample  
45 (SABER) to \$0.45–\$2.30 per sample depending on the scale of the experiment (Table 1); in  
46 both cases, the cost of these development reagents is a minor fraction of the overall cost of  
47 the SABER/pSABER ISH experiment. We have demonstrated that pSABER: a) is readily  
48 compatible with colorimetric detection and histopathological stains, b) can substantially  
49 amplify target signals >20x beyond conventional SABER while maintaining expected

1 subcellular localization patterns, c) can be multiplexed via solution exchange, d) is compatible  
2 with a broad range of optical systems including those commonly found in clinical labs, e) and  
3 can reveal detailed information about the spatial distribution of nucleic acid targets even on low  
4 numerical aperture and low magnification platforms. Given the simplicity, robustness and  
5 flexible readout options of the pSABER approach, we anticipate that it will serve as an enabling  
6 imaging technology in a wide set of clinical and research settings.

## 7 8 9 **Methods**

### 10 11 **Cell culture**

12 K29Mes human kidney mesangial cells<sup>30</sup> were obtained from M. Saleem (University of Bristol)  
13 and cultured in RPMI-1640 medium supplemented with 10% (vol/vol) FBS, 1x L-glutamine, 1x  
14 non-essential amino acids, ITS+ supplement, and 50 U/ml penicillin, and 50 µg /ml  
15 streptomycin. K29Mes cells were grown at 33°C (permissive temperature) and were then  
16 shifted to 37°C (nonpermissive temperature) before fixation causing degradation of the  
17 temperature sensitive SV40 T-antigen to promote growth arrest and differentiation. Prior to  
18 experiments, cells were either seeded on 22 x 22 mm #1.5 coverslips in 6-well plates at a  
19 density of about 100,000 cells per well or seeded on Ibidi 8-well chamber slides at a density of  
20 about 70,000 and kept at 37°C overnight to allow adherence to coverslips. Cells were then  
21 rinsed in 1x PBS, fixed in either 4% (wt/vol) paraformaldehyde in 1x PBS or 10% (vol/vol)  
22 neutral buffered formalin for 10 minutes at room temperature, then rinsed twice in 1x PBS.  
23 EY.T4<sup>34</sup> mouse embryonic fibroblast cells mouse embryonic fibroblast cells were grown in  
24 DMEM (ThermoFisher 10566016) supplemented with 15% (vol/vol) FBS (ThermoFisher  
25 A3160502), 50 U/ml penicillin, and 50 µg /ml streptomycin (ThermoFisher 15140122) 37°C in  
26 the presence of 5% CO<sub>2</sub>.

### 27 28 **Tissue**

29 All deidentified human kidney tissue samples used in experiments were from the renal cortex  
30 region of the kidney obtained through nephrectomies performed at the University of  
31 Washington hospitals with local institutional review board approval (STUDY00001297). Fresh  
32 tissue was fixed for a minimum of 8 hours-overnight in 10% (vol/vol) neutral buffered formalin  
33 followed by rinsing in H<sub>2</sub>O and storage in 70% EtOH at 4°C till paraffin embedding. After  
34 embedding, 5 µm sections were obtained and placed on positively-charged microscope slides.

### 35 36 **FISH probes**

37 Oligo probes targeting the human alpha satellite repeat, the human and mouse ITS1 RNA, the  
38 mouse 7SK RNA, and the mouse minor satellite repeat were purchased as individually column-  
39 synthesized DNA oligos from Integrated DNA Technologies. Probe sets targeting the human  
40 *ADAMTS1* mRNA, the human *UMOD* mRNA, and the mouse *Cbx5* mRNA were designed using  
41 PaintSHOP<sup>31</sup> and ordered in plate oligo or oPool format from Integrated DNA Technologies.  
42 The complex oligo library used to target Xp22.32 was purchased from Twist Biosciences and  
43 amplified and processed as described previously<sup>31</sup>. The sequences of the oligos probes used  
44 are listed in Supplementary Dataset 1.

### 45 46 **Primer exchange reaction**

47 To extend FISH probes into PER concatemers, 100 µl reactions were set up containing 1x  
48 PBS, 10mM MgSO<sub>4</sub>, 300 µM dNTP mix (dA, dC and dT only), 100 nM Clean.G hairpin, 40-600  
49 U/mL of Bst LF polymerase (New England Biolabs), 500 nM of hairpin, and water to 90 µl.

1 Reactions were incubated for 15 minutes at 37°C, then 10 µl of 10 µM of primer was added to  
2 each reaction and incubated at 37°C for 2 hours, followed 20 minutes at 80°C to heat-  
3 inactivate the polymerase. To check the success of extensions and concatemer lengths,  
4 samples (diluted in 2x Novex TBE-Urea sample buffer) and DNA ladders (Low Range and 100  
5 bp or 1 kb Plus, Thermo Fisher Scientific) were boiled at 95°C for 5 minutes then were run on  
6 10-15% TBE-Urea gels for 30-60 minutes at 70°C using a circulating water bath hooked up to  
7 the gel cassette. Reactions were dehydrated via vacuum evaporation for long-term storage (at  
8 room temperature) and resuspended in hybridization solutions for downstream F/ISH  
9 experiments.

10

### 11 **Colorimetric DNA pSABER in fixed tissue culture cells**

12 Fixed samples were permeabilized in 1x PBS with 0.1% (vol/vol) Triton X-100 for 10 minutes at  
13 room temperature, rinsed in 1x PBS, incubated in 0.5% (vol/vol) H<sub>2</sub>O<sub>2</sub> in 1x PBS for 10 minutes,  
14 rinsed twice with 1x PBS, treated with 0.1N HCl for 5 minutes and washed twice with 2x SSC  
15 plus 0.1% (vol/vol) Tween-20 (2x SSCT). Coverslips were incubated in 2x SSCT with 50%  
16 (vol/vol) formamide for 2 minutes at room temperature and again for 20 minutes at 60°C.  
17 Samples were then inverted onto 25 µl of primary hybridization solution made up of 2x SSCT,  
18 0.1% (vol/vol) Tween-20, 50% (vol/vol) formamide, 10% (wt/vol) dextran sulfate, 400 ng/µl of  
19 RNaseA, and 92 µl of dried PER reaction. Coverslips were placed in a humidified chamber,  
20 denatured at 78°C on a water-immersed heat block 3 minutes and then transferred to a  
21 benchtop air incubator for overnight incubation at 45°C. After hybridization with primary  
22 probes, samples were rinsed quickly in pre-warmed 2x SSCT before 4 rounds of 5-minute  
23 washes at 60°C and then 2 rounds of 2-minute washes in 2x SSCT at room temperature. For  
24 secondary hybridization (colorimetric detection), samples were rinsed in 1x PBS, incubated in  
25 blocking solution (1% wt/vol BSA and 0.1% vol/vol Tween-20 in 1x PBS), washed with 1x PBS  
26 twice, and inverted onto 25 µl of secondary hybridization solution consisting of 2x SSCT, 0.1%  
27 (vol/vol) Tween-20, 30% (vol/vol) formamide, 10% (wt/vol) dextran sulfate, and 100 nM HRP-  
28 oligo held at 37°C for 1 hour. Following secondary hybridization, coverslips were washed twice  
29 for 5 minutes in 1x PBS with 0.1% (vol/vol) Tween-20 at 37°C followed by a 5-minute wash in  
30 1x PBS at room temperature. To develop color, samples were inverted onto 25 µl of DAB  
31 solution (1 drop of DAB Chromogen plus 50 drops of DAB substrate—Abcam ab64238) for 30  
32 minutes, washed twice with tap water, counterstained with hematoxylin for 1 minute, rinsed  
33 with tap water twice, washed with 0.002% (vol/vol) ammonia water, and then washed in 70%,  
34 95% and 100% (vol/vol) ethanol for a 3–5 mins each. To mount coverslips, they were each  
35 dipped in xylene 5 times and inverted onto a microscope slide holding a few drops of  
36 CytoSeal-XYL mounting medium. Mounted coverslips were kept in a microscope slide case at  
37 room temperature prior to imaging.

38

### 39 **Colorimetric DNA pSABER on metaphase spreads**

40 Carrying out colorimetric DNA pSABER on human metaphase chromosome spreads was  
41 similar to the 'Colorimetric DNA pSABER in fixed tissue culture cells' protocol except for the  
42 steps taken right before primary probe hybridization. Slides with metaphase spreads were  
43 taken out of the -20°C freezer and denatured in 2x SSCT + 70% (vol/vol) formamide at 70°C  
44 for 3 minutes, followed by a 5-minute wash in ice-cold 70% (vol/vol) ethanol, in 90% (vol/vol)  
45 ethanol and in 100% ethanol and then allowed to air-dry before applying hybridization solution.

46

### 47 **Colorimetric RNA pSABER in fixed tissue culture cells**

48 Fixed samples were permeabilized in 1x PBS with 0.1% (vol/vol) Triton X-100 for 10 minutes at  
49 room temperature, rinsed in 1x PBS, incubated in 0.5% (vol/vol) H<sub>2</sub>O<sub>2</sub> in 1x PBS for 10 minutes,



1 rinsed twice with 1x PBS, washed once with 1x PBS containing 0.1% (vol/vol) Tween (PBST),  
2 and once with 2x SSCT. Samples were then inverted onto 25  $\mu$ l of primary hybridization  
3 solution made up of 2x SSCT, 0.1% (vol/vol) Tween-20, 10-40% (vol/vol) formamide, 10%  
4 dextran sulfate, and 92  $\mu$ l of dried PER reaction. Coverslips were placed in a humidified  
5 chamber, denatured at 60°C on a water-immersed heat block for 3 minutes and then  
6 transferred to a benchtop air incubator for overnight incubation at 42°C. After hybridization  
7 with primary probes, samples were rinsed quickly in pre-warmed 2x SSCT before 4 rounds of  
8 5-minute washes at 60°C and then 2 rounds of 2-minute 2x SSCT washes at room  
9 temperature. For secondary hybridization (colorimetric detection), samples were rinsed in 1x  
10 PBS, incubated in blocking solution (1% wt/vol BSA and 0.1% vol/vol Tween-20 in 1x PBS),  
11 washed with 1x PBS twice and inverted onto 25  $\mu$ l of secondary hybridization solution  
12 consisting of 2x SSCT, 0.1% (vol/vol) Tween-20, 30% (vol/vol) formamide, 10% (wt/vol)  
13 dextran sulfate and 100nM HRP-oligo and held at 37°C for 1 hour in the dark. Following  
14 secondary hybridization, coverslips were washed twice for 5 minutes in PBST at 37°C followed  
15 by a 5-minute wash in 1x PBS at room temperature. To develop color, samples were inverted  
16 onto 25  $\mu$ l of DAB solution (1 drop of DAB Chromogen plus 50 drops of DAB substrate for 30  
17 minutes, washed twice with tap water, counterstained with hematoxylin for 1 minute, rinsed  
18 with tap water twice, washed with 0.002% (vol/vol) ammonia water, and then washed in 70%,  
19 95% and 100% (vol/vol) ethanol for a few minutes each. To mount coverslips, they were each  
20 dipped in xylene 5 times and inverted onto a microscope slide holding a few drops of  
21 CytoSeal-XYL mounting medium for. Mounted coverslips were kept in a microscope slide case  
22 at room temperature prior to imaging.

23

#### 24 **Colorimetric RNA pSABER in FFPE tissue**

25 To deparaffinize FFPE sections, slides were placed in a slide rack and submerged in xylene  
26 twice for five minutes, incubated in 100% ethanol twice for 1 minute then removed and allowed  
27 to be air dried for 5 minutes at room temperature. To prepare FFPE tissue sections for *in situ*  
28 hybridization, pretreatment reagents from Advanced Cell Diagnostics (ACD) were used.  
29 Sections were incubated in 5–8 drops of ACD's hydrogen peroxide for 10 minutes at room  
30 temperature and rinsed with distilled water twice. The tissue slides were then submerged into  
31 the boiling 1x Target Retrieval solution from ACD for 10 minutes and immediately transferred to  
32 a staining dish containing distilled water, followed by another water rinse. Slides were washed  
33 in 100% ethanol quickly and allowed to be air dried. Lastly, sections were incubated with  
34 ACD's Protease Plus, placed in a humidified chamber inside an air incubator at 40°C for 40  
35 minutes and washed with distilled water twice. Pretreatment steps were followed by primary  
36 probe hybridization and all the following steps detailed in the protocol for 'Colorimetric RNA  
37 pSABER in fixed tissue culture cells' protocol.

38

#### 39 **Fluorescent RNA pSABER in fixed tissue culture cells**

40 Fixed cells that were grown on Ibidi 8-well chamber slides underwent the same steps  
41 described in the 'Colorimetric RNA pSABER in fixed tissue culture cells' protocol up to the  
42 wash prior to undergoing secondary hybridization. For the secondary hybridization 125  $\mu$ l of  
43 secondary hybridization solution consisting of 2x SSCT, 0.1% (vol/vol) Tween-20, 10% (wt/vol)  
44 dextran sulfate and 100nM HRP-oligo was added to the samples and held at 37°C for 1 hour in  
45 the dark. Cells in each well were then washed 3 times for 5 minutes in PBST at 37°C. To  
46 employ signal amplification via tyramide, fluorescent tyramide reagents that were purchased  
47 from Tocris were optimized and final concentrations of 480nM, 1.1  $\mu$ M, and 3.75  $\mu$ M for  
48 fluorescein, cy3 and cy5 tyramides were established respectively. To develop signal, 125  $\mu$ l of  
49 tyramide solution consisting of 1x PBS, 0.0015% (vol/vol) H<sub>2</sub>O<sub>2</sub>, and one of the fluorescent

1 tyramides was added to the samples for 10 minutes at room temperature. To quench enzyme  
2 activity, samples were washed 3 times for 5 minutes with a quenching solution containing 10  
3 mM sodium azide and 10 mM sodium ascorbate in PBST and 2 extra washes with PBST alone.  
4 Prior to being imaged, 125  $\mu$ l of SlowFade Gold Antifade Mountant with DAPI was added to  
5 each well.  
6

#### 7 **DNA SABER-FISH and Fluorescent DNA pSABER in fixed tissue culture cells**

8 DNA FISH was performed essentially as described previously<sup>28</sup>. Cells were grown on Ibidi 18-  
9 well chamber slides at a seeding density of ~7000 cells/ well in a mammalian tissue culture  
10 incubator and fixed in 4% (wt/vol) paraformaldehyde for 10 minutes. The samples were  
11 permeabilized in 1x PBS + 0.5% (vol/vol) Triton x-100 for 10 minutes at room temperature  
12 (hereafter RT), rinsed in 1x PBS + 0.1% Tween-20 (hereafter PBS-T) for 5 minutes, incubated in  
13 0.1N HCl for 5 minutes, rinsed with PBS-T, incubated in 3% (vol/vol) H<sub>2</sub>O<sub>2</sub> in PBS-T for 10  
14 minutes (pSABER only), rinsed twice with 2x SSC + 0.1% (vol/vol) Tween-20 (hereafter 2x  
15 SSCT), incubated in 2x SSCT + 50% (vol/vol) formamide for 2 minutes, incubated in 2x SSCT+  
16 50% (vol/vol) formamide at 60°C for 20 minutes on a water-immersed heat block, and  
17 denatured at 80°C for 3 minutes in a hybridization solution consisting of 2x SSC, 0.1% (vol/vol)  
18 Tween-20, 50% (vol/vol) formamide, 10% (wt/vol) dextran sulfate, 0.4 $\mu$ g/ $\mu$ l RNase A, and 100  
19 pmol of unpurified PER reaction. The slide was then held at 37°C overnight in a humidified  
20 chamber. On the next day, 4 washes' worth of 2x SSCT were pre-warmed to 60°C and the  
21 cells were rinsed twice with RT 2x SSCT. The cells were then rinsed 4x with the pre-warmed  
22 2xSSCT on a 60° heat block, with each rinse taking 5 minutes. This was followed by two quick  
23 RT rinses with 2x SSCT and three quick rinses in 1x PBS. The cells were then incubated at  
24 37°C for 1 hour in a secondary hybridization solution consisting of 0.1 $\mu$ M fluor oligos (SABER)  
25 or HRP-oligos (pSABER) in 1x PBS. During this hour, three washes' worth of PBS-T were pre-  
26 warmed to 37°C. After the secondary hybridization was complete, the cells were rinsed 3x in  
27 the pre-warmed PBS-T, with each wash taking 5 minutes. For pSABER, cells were then  
28 incubated for 10 minutes at RT in a labeling solution consisting of fluorescein tyramide (Torcis  
29 6456) diluted 1:50,000 from its 24 mM stock and 0.0015% (vol/vol) H<sub>2</sub>O<sub>2</sub> in PBS-T. pSABER  
30 development, the cells were rinsed 3x for 5 minutes each in a reaction quenching solution  
31 consisting of 10mM sodium ascorbate and 10mM sodium azide in PBS-T. Finally, the cells  
32 were rinsed twice in PBS-T and SlowFade Gold antifade mountant with DAPI was added.  
33

#### 34 **Fluorescent RNA pSABER in FFPE tissue**

35 FFPE tissue sections underwent the same deparaffinization and pretreatment steps detailed in  
36 the protocol for Colorimetric RNA pSABER in FFPE tissue. Following pretreatment incubations,  
37 tissue samples went through the same stages laid out in the protocol for 'Fluorescent RNA  
38 pSABER in fixed tissue culture cells', however, they did not get SlowFade Gold Antifade  
39 Mountant with DAPI at the end. Prior to imaging, tissue slices were stained with 0.1  $\mu$ g/mL  
40 DAPI (in 1x PBS) for 5 minutes and washed with 1x PBS. To reduce autofluorescence, the  
41 samples were then treated with 1x TruBlack Lipofuscin Autofluorescence Quencher (in 70%  
42 ethanol) for 1 minute taking care not to dry the tissue sections. Slides were washed 3 times  
43 with 1x PBS and coverslips were mounted using Prolong Gold Antifade Mountant.  
44

#### 45 **Exchange RNA pSABER in fixed tissue culture cells**

46 The steps are identical to the steps of the 'Fluorescent RNA pSABER in fixed tissue culture  
47 cells' protocol, but instead of adding the mountant with DAPI at the end, the samples were  
48 washed with 60% (vol/vol) formamide in PBST for 15 minutes at room temperature to remove  
49 the first round of HRP-oligo, followed by 2 washes with 1x PBS for 1 minute, another 2 washes

1 for 2 minutes and a final 5-minute wash. To enable another round of detection, samples were  
2 incubated with BSA blocking solution again, and got 125  $\mu$ l of the second HRP-oligo  
3 hybridization solution followed by all the steps detailed in the ‘Fluorescent RNA pSABER in  
4 fixed tissue culture cells’ protocol that came after secondary hybridization. At the end either  
5 another round of detection was performed or 125  $\mu$ l of SlowFade Gold Antifade Mountant with  
6 DAPI was added to each well prior to imaging. The following three tyramides were used:  
7 fluorescein at 1:50,000 from the 24 mM stock (Tocris 6456); Cy3 at 1:15,000 from the 16 mM  
8 stock (Tocris 6457); Cy5 (Tocris 6458) at 1:4,000 from the 15 mM stock.

## 9 10 **Microscopy**

11 Transmitted light microscopy of colorimetric pSABER samples was performed on an Olympus  
12 BX41 upright microscope using 20x Plan N.A. 0.25, 40x UPlan N.A. 0.75 or 60x Ach N.A. 0.80  
13 air objectives with images captured using a Leica DFC420 camera. Confocal imaging of  
14 fluorescent SABER and pSABER samples was performed using Yokogawa CSU-W1 SoRa  
15 spinning disc confocal attached to a Nikon Eclipse Ti-2 microscopy. Excitation light was  
16 emitted at 30% of maximal intensity from 405 nm, 488 nm, 561 nm, or 640 nm lasers housed  
17 inside of a Nikon LUNF 405/488/561/640NM 1F commercial launch. Laser excitation was  
18 delivered via a single-mode optical fiber into the into the CSU-W1 SoRa unit. Excitation light  
19 was then directed through a microlens array disc and a ‘SoRa’ disc containing 50  $\mu$ m pinholes  
20 and directed to the rear aperture of a 100x N.A. 1.49 Apo TIRF oil immersion objective lens by  
21 a prism in the base of the Ti2. Emission light was collected by the same objective and passed  
22 via a prism in the base of the Ti2 back into the SoRa unit, where it was relayed by a 1x lens  
23 (conventional imaging) or 2.8x lens (super-resolution imaging) through the pinhole disc and  
24 then directed into the emission path by a quad-band dichroic mirror (Semrock Di01-  
25 T405/488/568/647-13x15x0.5). Emission light was then spectrally filtered by one of four single-  
26 bandpass filters (DAPI: Chroma ET455/50M; ATTO 488: Chroma ET525/36M; ATTO 565:  
27 Chroma ET605/50M; Alexa Fluor 647: Chroma ET705/72M) and focused by a 1x relay lens onto  
28 an Andor Sona 4.2B-11 camera with a physical pixel size of 11  $\mu$ m, resulting in an effective  
29 pixel size of 110 nm (conventional) or 39.3 nm (super-resolution). The Sona was operated in  
30 16-bit mode with rolling shutter readout and exposure times of 70–300 ms. Automated slide-  
31 scanning microscopy was performed on a Keyence BZ-X800. Excitation light from the  
32 integrated white light source was emitted at 25% of maximal intensity, passed through the ‘ET  
33 DAPI’, ‘ET GFP’, ‘Cy3’, or ‘Cy5’ filter cube for excitation band filtering and was directed to the  
34 sample by a 10x N.A. 0.45 Plan Apo, 20x N.A. Plan Apo, or 40x N.A. 0.95 air objective lens.  
35 Emission light was collected by one of the objective lenses and directed into the microscope’s  
36 emission path by one of the filter cubes, after which it was spectrally filtered while exiting the  
37 filter cube and focused by a 1x relay lens onto an integrated CCD camera with a physical pixel  
38 size of 7.549  $\mu$ m, resulting in effective pixels sizes of 188.7 nm (40x), 377.4 nm (20x), or 754.9  
39 nm (10x). The CCD camera was operated in 14-bit mode without pixel binning and exposure  
40 times of 16.7–666.7 ms. Images were processed in ImageJ/Fiji<sup>36,37</sup> and Adobe Photoshop.

## 41 42 **Quantitative analysis of peak puncta intensities**

43 We developed an image analysis pipeline to detect and segment puncta from both SABER and  
44 pSABER experiments quantify their peak intensities. The pipeline is capable of loading .nd2  
45 image files containing channels with a nuclear stain (here DAPI) and fluorescent puncta,  
46 segmenting nuclei in 2D and detecting puncta inside the nuclei, and returning raw intensity  
47 values for each punctum. Each image is first loaded with the nd2reader python package, and  
48 DAPI / GFP channels are split for separate processing pathways. For the DAPI channel, 2D

1 segmentation was performed with the python package StarDist, specifically the  
2 “2D\_versatile\_fluo” pretrained model<sup>38,39</sup>. To generate more accurate segmentation results,  
3 nuclear segmentation was performed on a max-intensity projection which was downsampled  
4 by a factor of 16. The resulting segmentation mask was then upsampled to the original  
5 resolution. For the GFP channel, a maximum-intensity projection was generated and spot  
6 detection was performed using the *blob\_log* function from scikit-image<sup>40</sup>. Spot detection with  
7 *blob\_log* consisted of fitting a 2D Gaussian distribution to each punctum and returned the  
8 highest-intensity pixel as the 16-bit intensity of the spot. For SABER, sigma parameters were  
9 set as follows: threshold = 0.02, min\_sigma=0.001, max\_sigma=0.5, num\_sigma=20. For  
10 pSABER, sigma parameters were set as: min\_sigma=0.01, max\_sigma=1, num\_sigma=20.  
11 Detected spots were then filtered based on overlap with the nuclear segmentation mask. Data  
12 from each condition was aggregated and visualized with matplotlib. To quantify signal  
13 amplification, the cumulative distribution function for the SABER and pSABER spot intensities  
14 was generated, and the distributions were normalized to the SABER condition (median = 1).  
15 Signal amplification here was defined as the resulting median of the pSABER distribution.  
16  
17

## 18 **Code and Data Availability**

19 The source code for the automated analysis of peak puncta intensities as well as example  
20 input images is available at <https://github.com/beliveau-lab/SABER-Spot-Quant> under a MIT  
21 license. Additional primary microscopy data will be made available upon request.  
22

## 23 **Author Contributions**

24 S. Attar, S. Akilesh, and B.J.B. conceived the study. V.A.B. wrote and optimized software code.  
25 S. Attar, V.A.B., E.K.N., and A.F.T. performed experiments. S. Attar, V.A.B., S. Akilesh, and  
26 B.J.B. wrote the manuscript. All authors edited and approved the manuscript. D.M.S., J.S.,  
27 J.A.L., S. Akilesh, and B.J.B. supervised the work.  
28  
29

## 30 **Competing Interests**

31 S. Attar, A.F.T., D.M.S., S. Akilesh, and B.J.B. have filed a patent application covering  
32 pSABER. B.J.B. is listed as an inventor on patent applications related to the SABER  
33 technology.  
34  
35

## 36 **Acknowledgements**

37 The authors thank members of the Shechner, Shendure, Lieberman, Akilesh, and Beliveau labs  
38 for helpful discussion about this work. We thank N. Peters of the UW W.M. Keck Microscopy  
39 Center and D. Fong of Nikon for assistance with microscopy during the development of  
40 pSABER and S. Jiang for helpful advice about working with HRP in tissues. This work was  
41 supported by a Damon Runyon Dale F. Frey Breakthrough Award (32-19 to B.J.B.), the  
42 National Institutes of Health (under grants 1R35GM137916 to B.J.B., 1UM1HG011586 to J.S.  
43 and B.J.B., 1R01DK130386 to S. Akilesh, 1R01GM138799-01 to D.M.S.), the Andy Hill Cancer  
44 Research Endowment (under a COVID-19 Response Grant Award to B.J.B. and S. Akilesh),  
45 and the Diabetic Complications Consortium (under grant 19AU3987 to S. Akilesh and B.J.B.).  
46 This project was also supported in part by a Building Bridges Award to J.A.L. and S. Akilesh

1 from the Department of Laboratory Medicine and Pathology. A.F.T. was supported by NIH  
2 training grant T32GM007750.

3  
4

## 5 **References**

- 6
- 7 1. Pardue, M. L. & Gall, J. G. Molecular hybridization of radioactive DNA to the DNA of  
8 cytological preparations. *Proc. Natl. Acad. Sci. U. S. A.* **64**, 600–604 (1969).
  - 9 2. Riegel, M. Human molecular cytogenetics: From cells to nucleotides. *Genetics and*  
10 *Molecular Biology* vol. 37 194–209 Preprint at <https://doi.org/10.1590/S1415->  
11 [47572014000200006](https://doi.org/10.1590/S1415-47572014000200006) (2014).
  - 12 3. Raj, A., van den Bogaard, P., Rifkin, S. a., van Oudenaarden, A. & Tyagi, S. Imaging  
13 individual mRNA molecules using multiple singly labeled probes. *Nat. Methods* **5**, 877–879  
14 (2008).
  - 15 4. Solovei, I. *et al.* Spatial preservation of nuclear chromatin architecture during three-  
16 dimensional fluorescence in situ hybridization (3D-FISH). *Exp. Cell Res.* **276**, 10–23 (2002).
  - 17 5. Rosen, B. & Beddington, R. S. Whole-mount in situ hybridization in the mouse embryo:  
18 gene expression in three dimensions. *Trends Genet.* **9**, 162–167 (1993).
  - 19 6. Rudkin, G. T. & Stollar, B. D. High resolution detection of DNA-RNA hybrids in situ by  
20 indirect immunofluorescence [29]. *Nature* vol. 265 472–473 Preprint at  
21 <https://doi.org/10.1038/265472a0> (1977).
  - 22 7. Bauman, J. G. J., Wiegant, J., Borst, P. & van Duijn, P. A new method for fluorescence  
23 microscopical localization of specific DNA sequences by in situ hybridization of  
24 fluorochrome-labelled RNA. *Exp. Cell Res.* **128**, 485–490 (1980).
  - 25 8. Langer-Safer, P. R., Levine, M. & Ward, D. C. Immunological method for mapping genes  
26 on *Drosophila* polytene chromosomes. *Proc. Natl. Acad. Sci. U. S. A.* **79**, 4381–4385  
27 (1982).
  - 28 9. Rigby, P. W. J., Dieckmann, M., Rhodes, C. & Berg, P. Labeling deoxyribonucleic acid to  
29 high specific activity in vitro by nick translation with DNA polymerase I. *J. Mol. Biol.* **113**,  
30 237–251 (1977).
  - 31 10. Femino, a. M., Fay, F. S., Fogarty, K. & Singer, R. H. Visualization of single RNA transcripts  
32 in situ. *Science* **280**, 585–590 (1998).
  - 33 11. Yamada, N. A. *et al.* Visualization of fine-scale genomic structure by oligonucleotide-based  
34 high-resolution FISH. *Cytogenet. Genome Res.* **132**, 248–254 (2011).
  - 35 12. Boyle, S., Rodesch, M. J., Halvensleben, H. A., Jeddloh, J. A. & Bickmore, W. A.  
36 Fluorescence in situ hybridization with high-complexity repeat-free oligonucleotide probes  
37 generated by massively parallel synthesis. *Chromosome Res.* **19**, 901–909 (2011).
  - 38 13. Beliveau, B. J. *et al.* Versatile design and synthesis platform for visualizing genomes with  
39 Oligopaint FISH probes. *Proceedings of the National Academy of Sciences* **109**, 21301–  
40 21306 (2012).
  - 41 14. Lubeck, E., Coskun, A. F., Zhiyentayev, T., Ahmad, M. & Cai, L. Single-cell in situ RNA  
42 profiling by sequential hybridization. *Nature methods* vol. 11 360–361 (2014).

- 1 15. Chen, K. H., Boettiger, A. N., Moffitt, J. R., Wang, S. & Zhuang, X. RNA imaging. Spatially  
2 resolved, highly multiplexed RNA profiling in single cells. *Science* **348**, aaa6090 (2015).
- 3 16. Wang, S. *et al.* Spatial organization of chromatin domains and compartments in single  
4 chromosomes. *Science* **353**, 598–602 (2016).
- 5 17. Jensen, E. Technical Review: In Situ Hybridization. *Anat. Rec.* **297**, 1349–1353 (2014).
- 6 18. McNicol, A. M. & Farquharson, M. A. In situ hybridization and its diagnostic applications in  
7 pathology. *J. Pathol.* **182**, 250–261 (1997).
- 8 19. Player, A. N., Shen, L. P., Kenny, D., Antao, V. P. & Kolberg, J. A. Single-copy gene  
9 detection using branched DNA (bDNA) in situ hybridization. *J. Histochem. Cytochem.* **49**,  
10 603–611 (2001).
- 11 20. Wang, F. *et al.* RNAscope: A novel in situ RNA analysis platform for formalin-fixed,  
12 paraffin-embedded tissues. *J. Mol. Diagn.* **14**, 22–29 (2012).
- 13 21. Beliveau, B. J. *et al.* Single-molecule super-resolution imaging of chromosomes and in situ  
14 haplotype visualization using Oligopaint FISH probes. *Nat. Commun.* **6**, 7147 (2015).
- 15 22. Choi, H. M. T. *et al.* Programmable in situ amplification for multiplexed imaging of mRNA  
16 expression. *Nat. Biotechnol.* **28**, 1208–1212 (2010).
- 17 23. Rouhanifard, S. H. *et al.* ClampFISH detects individual nucleic acid molecules using click  
18 chemistry-based amplification. *Nat. Biotechnol.* (2018) doi:10.1038/nbt.4286.
- 19 24. Dardani, I. *et al.* ClampFISH 2.0 enables rapid, scalable amplified RNA detection in situ.  
20 *Nat. Methods* **19**, 1403–1410 (2022).
- 21 25. Kerstens, H. M., Poddighe, P. J. & Hanselaar, a. G. A novel in situ hybridization signal  
22 amplification method based on the deposition of biotinylated tyramine. *J. Histochem.*  
23 *Cytochem.* **43**, 347–352 (1995).
- 24 26. Schulte-Merker, S., Ho, R. K., Herrmann, B. G. & Nüsslein-Volhard, C. The protein product  
25 of the zebrafish homologue of the mouse T gene is expressed in nuclei of the germ ring  
26 and the notochord of the early embryo. *Development* **116**, 1021–1032 (1992).
- 27 27. Lizardi, P. M. *et al.* Mutation detection and single-molecule counting using isothermal  
28 rolling-circle amplification. *Nature Genetics* vol. 19 225–232 Preprint at  
29 <https://doi.org/10.1038/898> (1998).
- 30 28. Kishi, J. Y. *et al.* SABER amplifies FISH: enhanced multiplexed imaging of RNA and DNA in  
31 cells and tissues. *Nat. Methods* (2019) doi:10.1038/s41592-019-0404-0.
- 32 29. Kishi, J. Y., Schaus, T. E., Gopalkrishnan, N., Xuan, F. & Yin, P. Programmable  
33 autonomous synthesis of single-stranded DNA. *Nat. Chem.* (2017)  
34 doi:10.1038/nchem.2872.
- 35 30. Sarrab, R. M. *et al.* Establishment of conditionally immortalized human glomerular  
36 mesangial cells in culture, with unique migratory properties. *Am. J. Physiol. Renal Physiol.*  
37 **301**, F1131-8 (2011).
- 38 31. Hershberg, E. A. *et al.* PaintSHOP enables the interactive design of transcriptome- and  
39 genome-scale oligonucleotide FISH experiments. *Nat. Methods* **18**, 937–944 (2021).
- 40 32. Rouquette, J., Choesmel, V. & Gleizes, P.-E. Nuclear export and cytoplasmic processing  
41 of precursors to the 40S ribosomal subunits in mammalian cells. *EMBO J.* **24**, 2862–2872

- 1 (2005).
- 2 33. Uhlén, M. *et al.* Proteomics. Tissue-based map of the human proteome. *Science* **347**,  
3 1260419 (2015).
- 4 34. Yildirim, E., Sadreyev, R. I., Pinter, S. F. & Lee, J. T. X-chromosome hyperactivation in  
5 mammals via nonlinear relationships between chromatin states and transcription. *Nat.*  
6 *Struct. Mol. Biol.* **19**, 56–61 (2011).
- 7 35. Prasanth, K. V. *et al.* Nuclear organization and dynamics of 7SK RNA in regulating gene  
8 expression. *Mol. Biol. Cell* **21**, 4184–4196 (2010).
- 9 36. Schneider, C. A., Rasband, W. S. & Eliceiri, K. W. NIH Image to ImageJ: 25 years of image  
10 analysis. *Nat. Methods* **9**, 671–675 (2012).
- 11 37. Schindelin, J. *et al.* Fiji: an open-source platform for biological-image analysis. *Nat.*  
12 *Methods* **9**, 676–682 (2012).
- 13 38. Schmidt, U., Weigert, M., Broaddus, C. & Myers, G. Cell Detection with Star-Convex  
14 Polygons. in *Medical Image Computing and Computer Assisted Intervention – MICCAI*  
15 *2018* 265–273 (Springer International Publishing, 2018).
- 16 39. Weigert, Schmidt, Haase, Sugawara & Myers. Star-convex Polyhedra for 3D Object  
17 Detection and Segmentation in Microscopy. in *2020 IEEE Winter Conference on*  
18 *Applications of Computer Vision (WACV)* vol. 0 3655–3662 (2020).
- 19 40. van der Walt, S. *et al.* scikit-image: image processing in Python. *PeerJ* **2**, e453 (2014).

20

## 21 **Figure Legends**

22

23 **Fig. 1 | Schematic overview of pSABER.** *In vitro* extended primary oligo probes are applied to  
24 samples and hybridized *in situ* to DNA or RNA targets, facilitating the recruitment of a  
25 secondary oligo conjugated with horseradish peroxidase (HRP) that can locally catalyze the  
26 deposition of colorimetric or fluorescent labels.

27

28 **Fig. 2 | pSABER enables colorimetric detection of nucleic acid targets.** **a**, Visualization of  
29 the *ADAMTS1* mRNA in human K29Mes cells. **b**, Visualization of alpha satellite DNA in mRNA  
30 in human K29Mes cells. **c**, Visualization of a 200 kb genomic interval within Xp22.32 on primary  
31 human metaphase chromosome spreads. **d**, Visualization of ribosomal RNA internal  
32 transcribed spacer 1 (ITS1) region in deidentified primary human paraffin fixed, formalin  
33 embedded (FFPE) kidney tissue sections. **e**, Visualization of the *UMOD* mRNA in deidentified  
34 primary human FFPE kidney tissue sections. A no primary probe negative control image  
35 processed in parallel to each sample is shown to the left of each pSABER image. Scale bars,  
36 20  $\mu\text{m}$  (insets) or 50  $\mu\text{m}$  (fields of view). MD = macula densa. TALH = thock ascending loop of  
37 Henle.

38

39 **Fig. 3 | Fluorescent pSABER visualizes nucleic acid targets in cells and tissues.** **a**, DNA  
40 (DAPI, left), fluorescent pSABER targeting the ribosomal RNA internal transcribed spacer 1  
41 (ITS1) region performed in EY.T4 mouse embryonic fibroblasts (MEFs) (center), and a  
42 composite image (right). **b**, DNA (DAPI, left), fluorescent pSABER targeting the 7SK RNA  
43 performed in EY.T4 MEFs (center), and a composite image (right). **c**, DNA (DAPI, left),  
44 fluorescent pSABER targeting the *Cbx5* mRNA performed in EY.T4 MEFs (center), and a

1 composite image (right). **d**, DNA (DAPI, left), a no primary probe control for pSABER performed  
2 in EY.T4 MEFs (center), and a composite image (right). **e**, DNA (DAPI, left), fluorescent pSABER  
3 targeting ITS1 performed in deidentified primary human paraffin fixed, formalin embedded  
4 (FFPE) kidney tissue sections (center), and a composite image (right). **f**, DNA (DAPI, left), a no  
5 primary probe control for pSABER performed in deidentified primary human FFPE kidney  
6 tissue sections (center), and a composite image (right). Each set of images is presented at the  
7 indicated high (top) and low (bottom) contrast settings to allow for visual comparisons between  
8 signals occupying different portions of the 16-bit dynamic range (0–65535). Images are  
9 maximum projections in Z. Scale bars, 10  $\mu\text{m}$ .

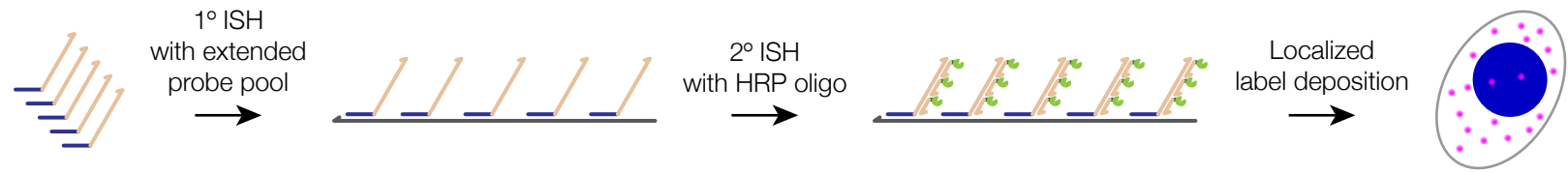
10  
11 **Fig. 4 | pSABER robustly amplifies fluorescent signals *in situ*.** **a**, Representative images of  
12 DNA FISH targeting the mouse minor satellite repeat in EY.T4 mouse embryonic fibroblasts  
13 visualized by SABER (left) or pSABER (right). Outlines of nuclei segmented using the DAPI  
14 signal (yellow, dashed line) are overlaid on all images. Each image is presented at the indicated  
15 high (top) and low (bottom) contrast settings to allow for visual comparisons between signals  
16 occupying different portions of the 16-bit dynamic range (0–65535). **b**, Distributions of the peak  
17 pixel intensity of each segmented puncta (see Methods). **c**, Normalized empirical cumulative  
18 distributions of the peak pixel intensity of each segmented puncta showing fold-enhancement  
19 over SABER, with vertical dashed lines corresponding to medians. A similar value of fold-  
20 enhancement was obtained comparing means (25.1x enhancement, medians; 21.3x  
21 enhancement, means).  $n_{\text{SABER}} = 5,171$  puncta;  $n_{\text{pSABER}} = 5,770$  puncta. Scale bars, 10  $\mu\text{m}$ .

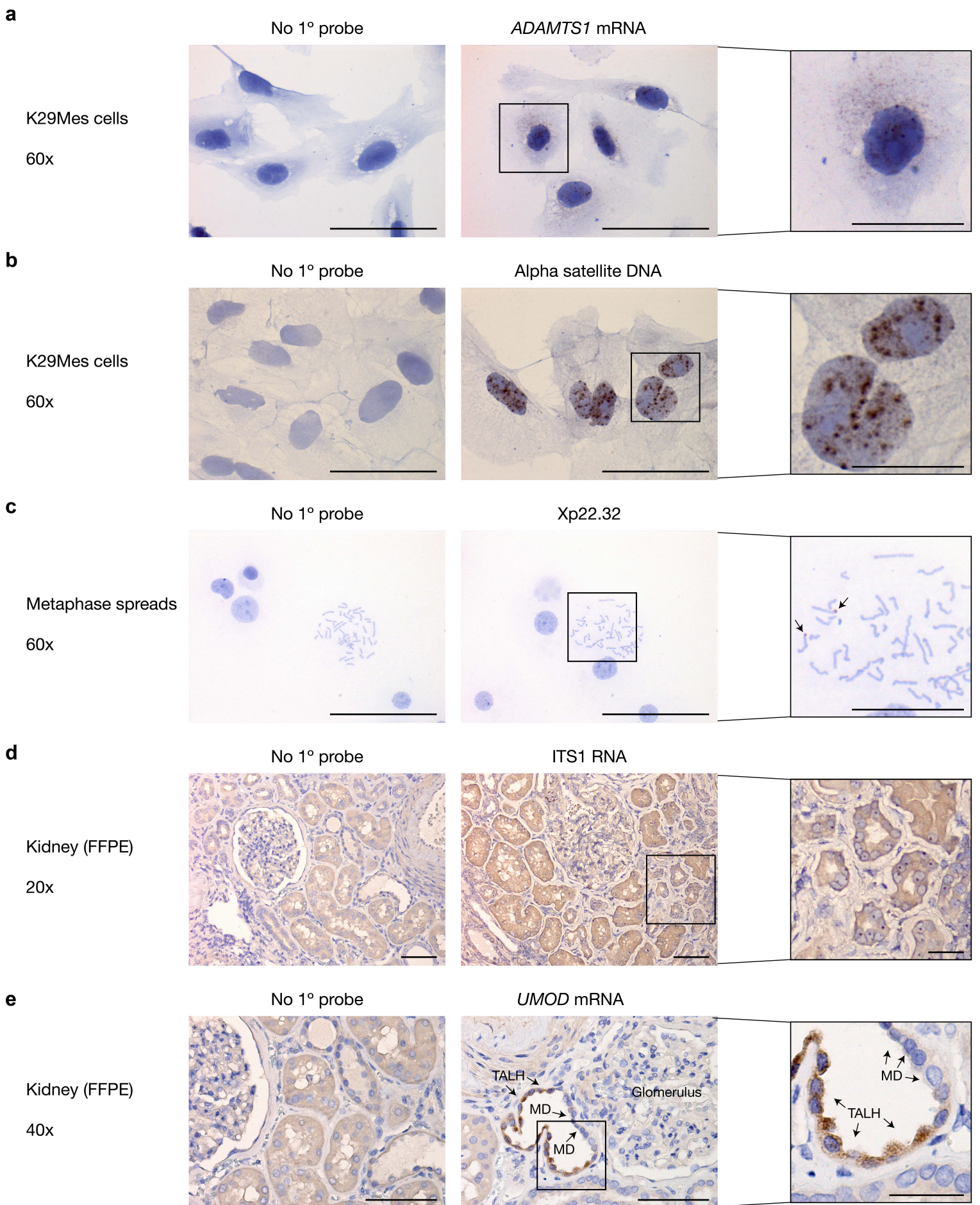
22  
23 **Fig. 5 | Exchange-pSABER enables highly amplified and multiplexed imaging.** **a**,  
24 Schematic overview of Exchange-pSABER depicting sequential rounds of hybridization with an  
25 HRP-oligo, development, displacement, and re-hybridization. **b**, 3 color Exchange-pSABER  
26 experiment in EY.T4 mouse embryonic fibroblasts targeting the *Cbx5* mRNA (round 1, Cy5,  
27 top), the 7SK RNA (round 2, Cy3, middle), and the ribosomal RNA internal transcribed spacer 1  
28 (ITS1) region (round 3, fluorescein, bottom). **c**, A composite image of the 3-color Exchange-  
29 pSABER experiment depicted in panel b taken using a SoRA CSU-W1 super-resolution  
30 spinning disc microscope. **d**, Composite images of the 3-color Exchange-pSABER experiment  
31 depicted in panel b taken using an automated slide-scanning microscope using 10x (left), 20x  
32 (center), and 40x (right) air objectives. Images are maximum projections in Z (a–c) or single Z  
33 slices (d). Scale bars, 10  $\mu\text{m}$  (a–c, fields of view), 20  $\mu\text{m}$  (d, insets), or 100  $\mu\text{m}$  (d, fields of view).

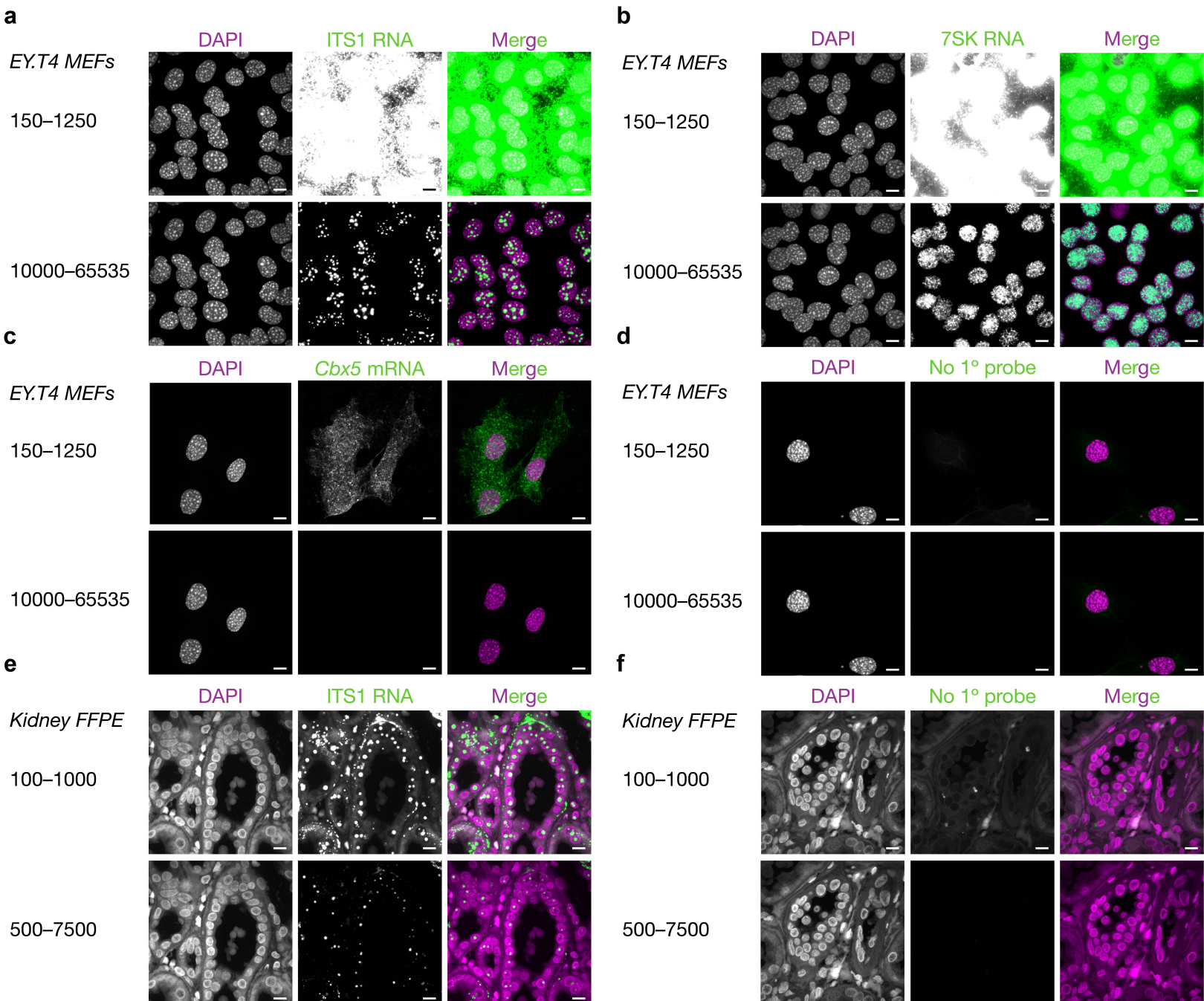
34  
35 **Table 1 | Cost comparison of visualization reagents for SABER and pSABER.** The cost per  
36 slide (center) and per imaging chamber slide well (right) are given for the key reagents needed  
37 to visualize SABER and pSABER.

38  
39 **Fig. S1 | Comparison of SABER and pSABER on a slide-scanning microscope.** **a**, SABER  
40 (left) and pSABER (right) visualization of mouse major satellite DNA imaged using a 10x air  
41 objective. **b**, SABER (left) and pSABER (right) visualization of mouse major satellite DNA  
42 imaged using a 20x air objective. **c**, SABER (left) and pSABER (right) visualization of mouse  
43 major satellite DNA imaged using a 10x air objective. Each image is presented at the indicated  
44 high (top) and low (bottom) contrast settings to allow for visual comparisons between signals  
45 occupying different portions of the 16-bit dynamic range (0–65535). Images are maximum  
46 projections in Z. Scale bars, 20  $\mu\text{m}$  (insets) or 100  $\mu\text{m}$  (fields of view).

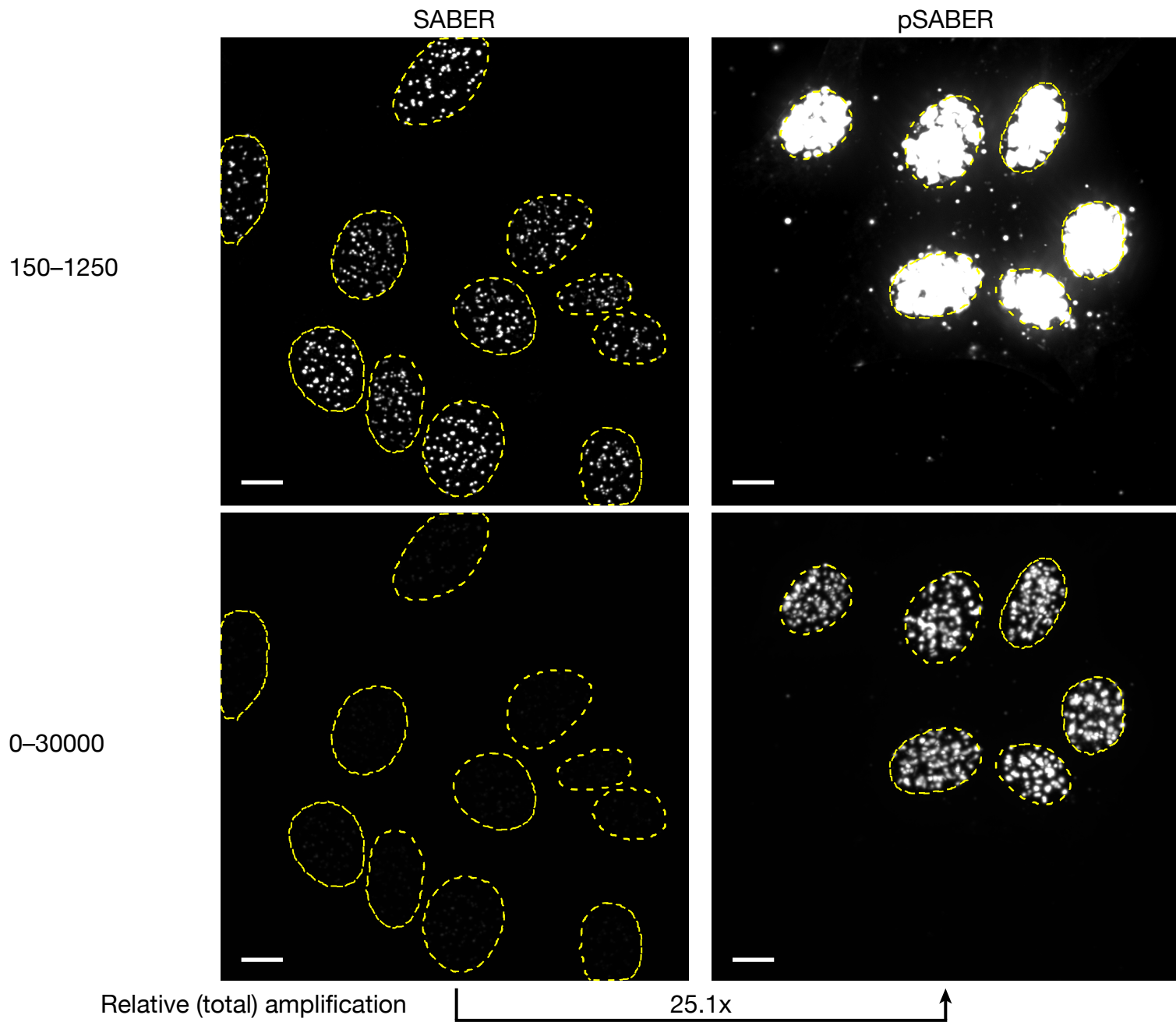




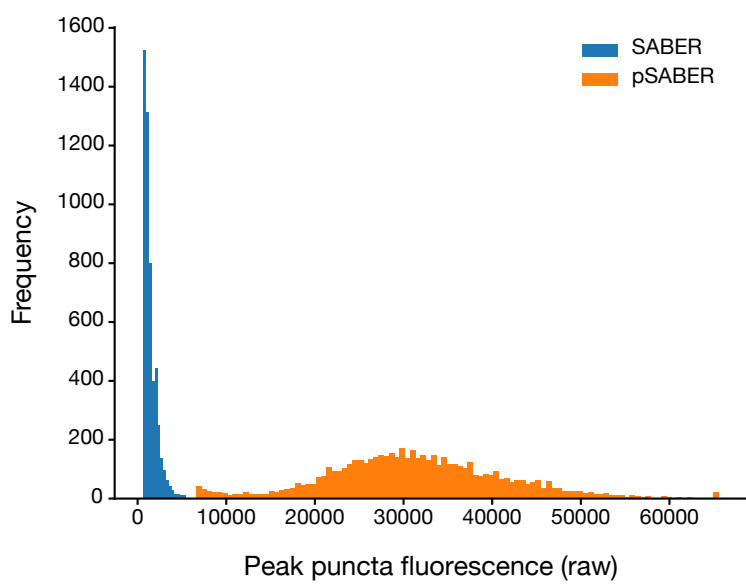




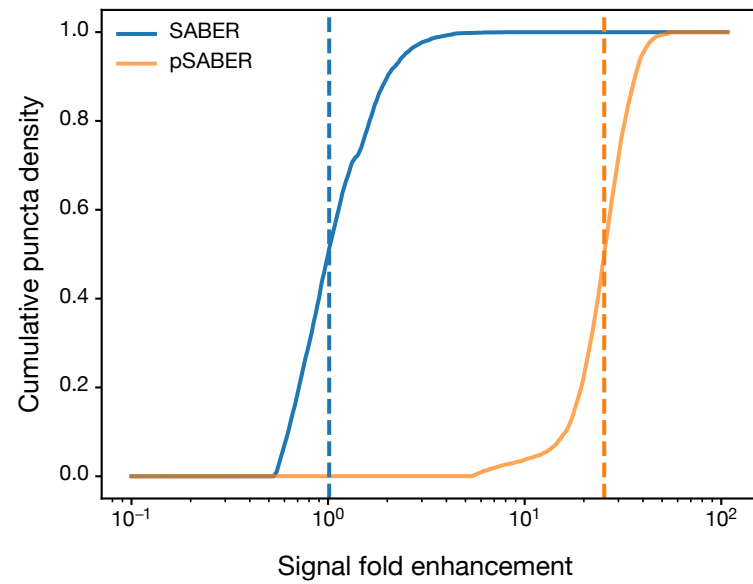
a

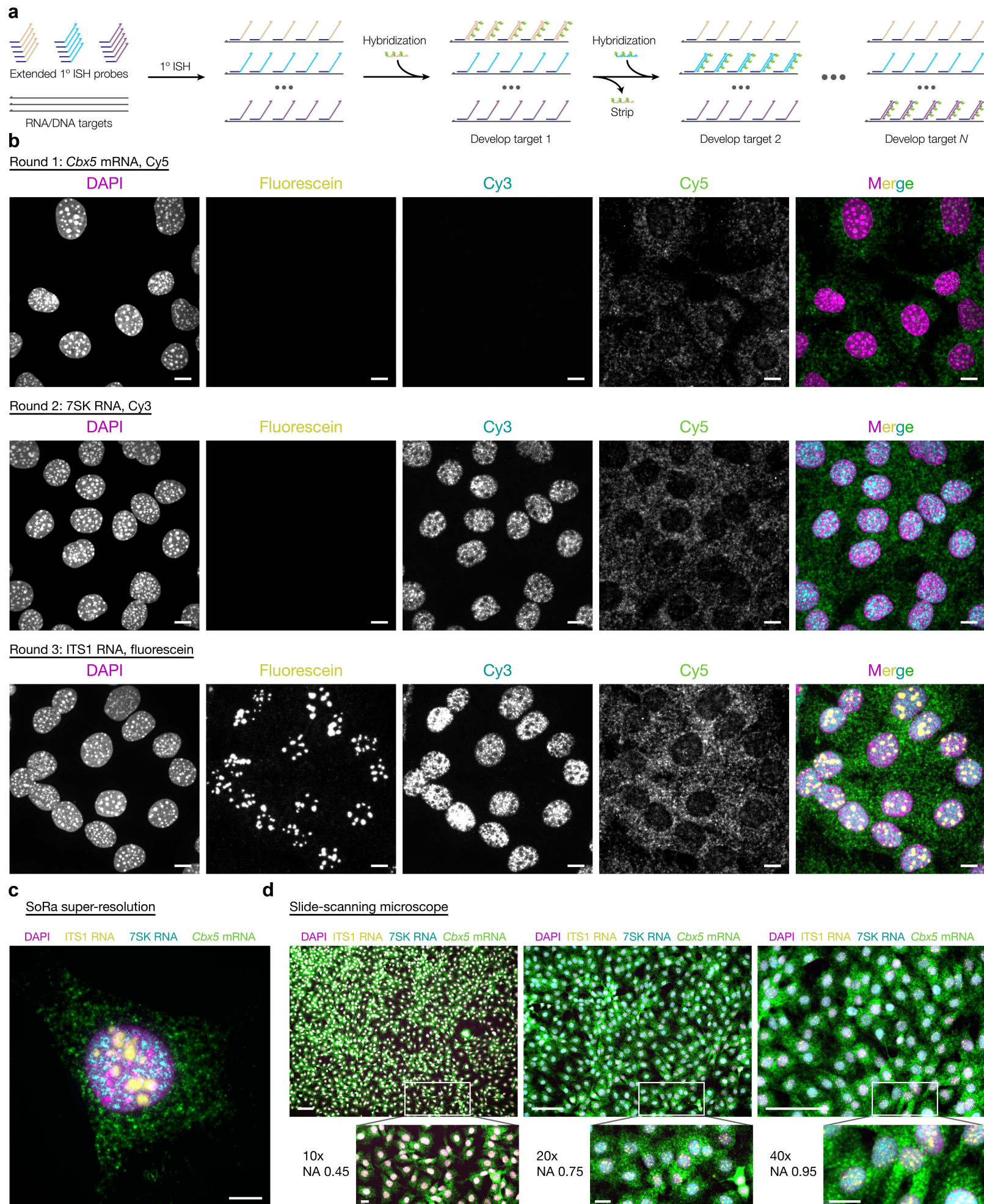


b



c





<b>Reagent</b>	<b>Cost per slide (25 <math>\mu</math>l)</b>	<b>Cost per well (125 <math>\mu</math>l)</b>
Fluor-oligo (SABER)	\$0.11	\$0.57
HRP oligo (pSABER)	\$0.44	\$2.22
Tyramide fluor (pSABER)	\$0.01	\$0.07

**Table 1**

